Med Chem Res (2010) 19:551–564
DOI 10.1007/s00044-009-9212-x

MEDICINAL CHEMISTRY RESEARCH

ORIGINAL RESEARCH

Synthesis, X-ray structure and antiproliferative activity of 3-benzylthio-4-propargylselenoquinoline

Stanislaw Boryczka · Maria Jastrzebska · Maria Nowak · Joachim Kusz · Roman Wrzalik · Joanna Wietrzyk · Małgorzata Matyja

Received: 23 December 2008 / Accepted: 15 April 2009 / Published online: 27 May 2009

Abstract Synthesis, antiproliferative activity and the X-ray single-crystal structure of the 3-benzylthio-4-propargylselenoquinoline are described. The title compound belongs to the group of the acetylenic derivatives of thioquinolines, which have been intensively investigated as a source of new anticancer agents. The comparative study regarding the X-ray structure, the molecular electrostatic potential analysis, and structure-activity relationship for the title compound and the 3-methylthio-4-propargylthioquinoline and 3-methylthio-4-propargylselenoquinoline are presented.

Keywords Structure-activity relationship · Antiproliferative activity · Electrostatic potential

S. Boryczka · M. Matyja
Department of Organic Chemistry, Faculty of Pharmacy, Medical University of Silesia, 41-200 Sosnowiec, Jagiellonska 4, Poland

M. Jastrzebska (✉)
Department of Radioisotope Diagnostics and Radiopharmaceuticals, Faculty of Pharmacy, Medical University of Silesia, 41-200 Sosnowiec, Jagiellonska 4, Poland
e-mail: maja@sum.edu.pl

M. Nowak · J. Kusz
Institute of Physics, Department of Physics of Crystals, University of Silesia, Uniwersytecka 4, 40-007 Katowice, Poland

R. Wrzalik
Department of Biophysics and Molecular Physics, Institute of Physics, University of Silesia, Uniwersytecka 4, 40-007 Katowice, Poland

J. Wietrzyk
Department of Experimental Oncology, Ludwik Hirszfeld Institute of Immunology and Experimental Therapy, Polish Academy of Sciences, Weigla 12, Wrocław, Poland

BIRKHÄUSER

Introduction

Acetylenic derivatives of thioquinolines are an important class of compounds that has attracted increasing attention as a source of new anticancer agents. The synthetic methods for their preparation are of interest especially with regard to the synthesis of biologically active enediyne antitumor antibiotics or similar model molecules (Grissom *et al.*, 1996; Jones and Found, 2002; Nicolaou and Dai, 1991; Gredicak and Jeric, 2007).

Recently, we have reported a simple and efficient method for the synthesis of thioquinolines, which possess the S, Se-acetylenic groups. It has been found that Se-acetylenic thioquinolines are more active in vitro than S-acetylenic derivatives against a broad panel of human and murine cancer cell lines with ID_{50} values comparable to that of referential anticancer drug, cisplatin (Boryczka *et al.*, 2002a, b; Mól *et al.*, 2006, 2008). The chemical and physical properties of Se are similar to those of sulfur, but the biochemistry differs in at least two respects that distinguish them in biological systems (Aboul-Fadl, 2005). First, in biological systems selenium compounds are metabolized to more reduced states, whereas sulfur compounds are metabolized to more oxidized states. Second, selenols are more acidic than thiols, and they are readily oxidized. In general, organoselenium compounds are more reactive than their sulfur analogues due to weaker C–Se bond than the C–S bond. These properties can be involved in higher activity of the Se-compounds against cancer cells than S-derivatives (Aboul-Fadl, 2005).

Apart from the synthesis and interest in the anticancer activity, these compounds are of relevance in the context of intermolecular interactions and the structure-activity relationship. The terminal alkyne group is expected to form C≡C–H···X hydrogen bond, with X being one of the potential hydrogen-bond acceptors of the molecule. Recently, we reported the crystal structures of 3-methylthio-4-propargylthioquinoline **1** and 3-methylthio-4-propargylselenoquinoline **2,** which contain an unusually short C≡C–H···N hydrogen bonds with distances H···N = 2.28 Å, C···N = 3.305 Å and H···N = 2.17 Å, C···N = 3.225 Å, respectively (Boryczka *et al.*, 2000a, 2001, 2002b). It also has been observed that compound **2** is more cytotoxic than **1**, with ID_{50} values ranging from 0.6 to 2.5 μg/ml (Table 1), against human cancer cell lines: lung cancer (A549), colon cancer (SW707), bladder cancer (HCV29T), breast cancer (T47D) (Boryczka *et al.*, 2002a, b). It is well known that formation of hydrogen bonds and lipophilicity play an important role in several

Table 1 Hydrogen bond distances and antiproliferative activity in vitro of propargyl thioquinolines **1–3** against the human cancer cell lines

Compound	Hydrogen bond distances (Å)		Cell line/ID_{50} (μg/ml)			
	H···N	C···N	A549	SW707	HCV29T	T47D
1*	2.28	3.305	6.8 ± 1.7	18.4 ± 2.2	17.6 ± 1.6	5.7 ± 1.1
2*	2.17	3.225	–	2.5 ± 1.6	0.6 ± 1.6	1.8 ± 1.4
3	Lack		>100	>100	>100	>100
Cis-platin			–	2.3 ± 1.1	0.7 ± 1.0	2.1 ± 1.8

* Boryczka *et al.*, 2002a, b

ADME aspects, which are adsorption, distribution, metabolism, and excretion in biological systems (Gensmantel, 2001). It was argued that the activity of compound **2** can be attributed to the presence of a propargylseleno group in the context of its very short intermolecular interactions.

To study the influence of the intermolecular interactions of the propargyl group on the cytotoxic activity of this class of compounds, we have prepared 3-benzylthio-4-propargylselenoquinoline **3**. Formation of the short hydrogen bonds could be a favorable event in the course of antiproliferative activity of the compounds being tested; however, this suggestion needs strong experimental verification.

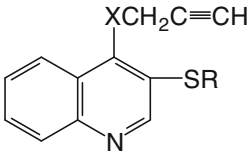

1. X = S, R = Me

2. X = Se, R = Me

3. X = Se, R = CH_2Ph

It also is of interest to examine the correlation between the antiproliferative activity of propargyl thioquinoline compounds and their reactive behavior predicted by the molecular electrostatic potential (MEP) analysis. The MEP can be particularly useful as an indicator of the sites of a molecule, to which an approaching electrophile is initially attracted (Murray *et al.*, 1991; Politzer *et al.*, 1985; Weiner *et al.*, 1982).

Results and discussion

Chemistry

The 3-benzylthio-4-propargylselenoquinoline **3** was synthesized by nucleophilic displacement of chloride in the corresponding 4-chloro-3-benzylthioquinolines **4** by selenourea in ethanol and subsequent S-alkylation of sodium salt **4-B** with propargyl bromide (Scheme 1) according to the reported method (Boryczka *et al.*, 2002a, b). Compound **4** was obtained following procedures described by Maślankiewicz and Boryczka (1993).

X-ray structure

The title compound (**3**) crystallizes in the centrosymmetric space group $P2_1/c$ with one molecule in the asymmetric unit cell. The refined molecule and the atomic numbering scheme are shown in Fig. 1. The crystal packing and selected geometric parameters are presented in Fig. 2 and Table 2, respectively.

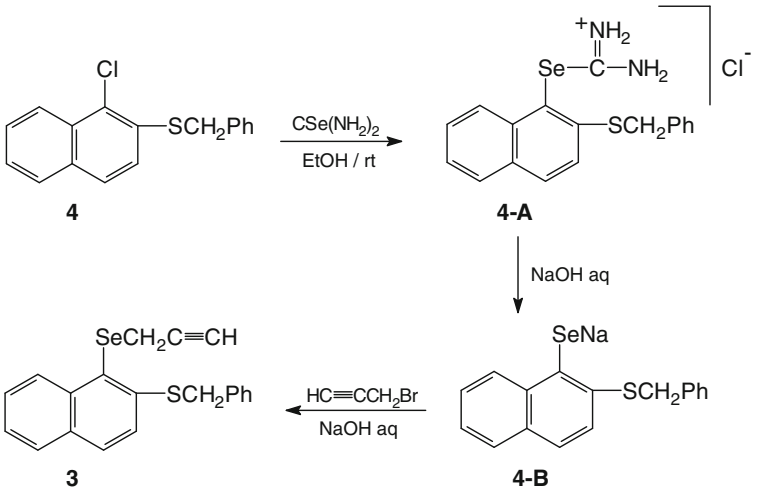

Scheme 1 Synthesis of 3-benzylthio-4-propargylselenoquinoline 3

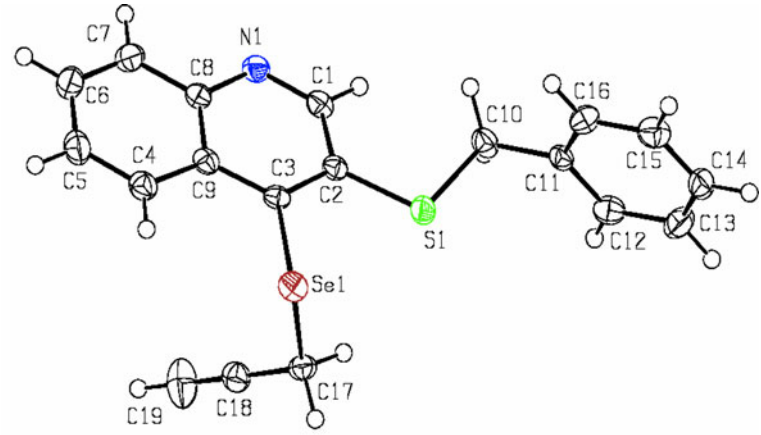

Fig. 1 View of the molecule **3** showing the atom-labeling scheme. Displacement ellipsoids are drawn at the 50% probability level and H atoms are shown as small spheres of arbitrary radii

The heterocyclic and carbocyclic rings of the quinoline core are, separately, essentially planar. The r.m.s. deviations of an atom from the best fit planes describing the rings are −0.0118 Å and 0.0020 Å, respectively. Because the angle between the planes of these rings is only 1.06(10)°, the quinoline core as a whole is nearly planar with r.m.s. deviations from the mean core plane of 0.0106 Å. The molecular dimensions in the quinoline core show the usual values reflecting in the heterocyclic ring somewhat more marked alternation of single- and double-bond character, e.g., the short N1–C1 and the longer N1–C8 bonds, the short C2–C3 and long C3–C9. They are comparable with similar structures: CSD refcode: ASAFUV

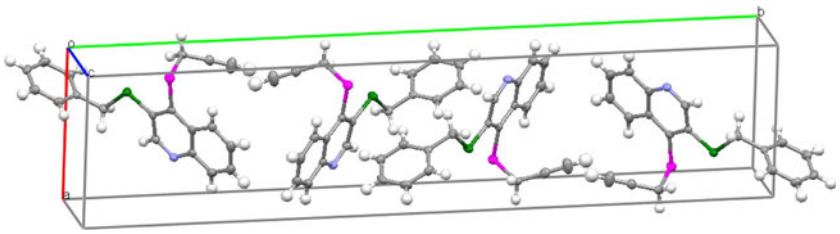

Fig. 2 The crystal packing of the compound **3**, viewed approximately along [001]

Table 2 Selected geometric parameters (Å, °) for compound **3**

N1–C1	1.307(2)	Se1–C3	1.929(2)
N1–C8	1.373(2)	Se1–C17	1.970(2)
S1–C2	1.757(2)	C17–C18	1.436(2)
S1–C10	1.821(2)	C18–C19	1.171(3)
C10–C11	1.508(2)	C19–H19	0.95
S1–Se1	3.198(8)		
C1–N1–C8	117.80(15)	C2–C3–Se1	119.82(13)
C1–C2–S1	123.14(13)	C9–C3–Se1	120.87(12)
C3–C2–S1	119.02(13)	C3–Se1–C17	96.54(7)
C2–S1–C10	104.84(8)	Se1–C17–C18	112.65(12)
S1–C10–C11	106.54(11)		
N1–C1–C3–S1	−177.35(11)	C1–C2–C3–Se1	177.72(12)
C1–C2–S1–C10	11.57(16)	C2–C3–Se1–C17	−72.25 (14)
C2–S1–C10–C11	158.72(12)	C3–Se1–C17–C18	−63.15 (14)
S1–C10–C11–C12	93.56(17)	S1–C2–C3–Se1	−2.12 (18)

(Duann *et al.*, 2003); CSD refcode: EDAVUA (Davies and Bond, 2001); CSD refcode: BAPBOK (Skrzypek and Suwinska, 2002); CSD refcode: FOCYUS (Fitchett *et al.*, 2005); CSD, Version 5.28; Conquest, Version 1.9 (Allen, 2002).

The triple-bond distance C18–C19 equals 1.171(3) Å and is shorter than that found previously in **1** and **2** (1.181(4) Å and 1.183 Å, respectively).

The length of the bonds C3–Se1 and Se1–C17 are equal to 1.929(2) Å and 1.970(2) Å, respectively, and they are similar to those in compound **2**. The selenium bond angle C3–Se1–C17 is 96.54(7)° and corresponds to quinolinyl–selenium bond angle present in compound **2** (95.84°). The C3–Se1 bond is nearly coplanar with the ring system, but the Se1–C17 bond, involving the propargyl group, is rotated almost perpendicularly out of the quinoline plane. The dihedral angle C2–C3–Se1–C17 is −72.25(14)° and this angle is smaller compared with compound **2** (−103.95) (Boryczka *et al.*, 2001). The propargyl group is pointing out of quinoline plane. The dihedral angle C3–Se1–C17–C18 is −63.15(14)° and it is smaller than in **2** (176.35°) (Boryczka *et al.*, 2001). This situation is similar to that observed for the orientation of propargyl groups in the crystal structure of the bis(4-propargyloxy-3-quinolylthio)methane (Boryczka *et al.*, 2000b), but it has different orientation to that

observed in **1** and **2**, where the propargyl group is oriented parallel to the C3–Se(S) bonds (Boryczka *et al.*, 2000a, 2001). This conformation about the Se1–C17 bond in **3** causes such position of the acetylenic hydrogen atom H19 that it is not favorable for C–H···N intermolecular hydrogen bonding.

The length of the bond C2–S1 is equal to 1.757(2) Å and is similar to those found earlier in compounds **1** and **2** (Boryczka *et al.*, 2000a, b, 2001). The bond length of S1–C10 is 1.821(2) Å and is close to the $C_{aliphatic}$ – S bonds (Mott and Barany, 1984). The sulfur bond angle C2–S1–C10 is 104.84(8)° and corresponds to the quinolinyl–sulfur bond angle of 103.79° and 103.25° in the sulfide **1** and **2**, respectively (Boryczka *et al.*, 2000a, b, 2001).

The quinoline ring also is coplanar with the central C–S bond (maximum out of plane distance is equal to 0.0242 Å). The torsion angle about this bond is 158.72 (12)°. The mean plane through benzyl group is twisted by 80.99(5)° with respect to the thioquinoline plane.

The S1–Se1 distance is equal to 3.198(1) Å and is less than the sum of the van der Waals radii of the sulfur and selenium atoms, which equals 3.85 Å (Bondi, 1964). The characteristic feature of the intramolecular nonbonded 1,4 S···Se contact in **3** is that the S1 and Se1 atoms are held in a nearly coplanar environment containing S1, C2, C3, and Se1, which form a four-member quasi-ring by a S1···Se1 interaction with a deviation of Se1 of 0.0045(4)Å. Also the arrangement of C10–S1···Se1 atoms is almost linear, the angle C10–S1···Se1 is equal to 164.92(6)° and it promotes the 1,4 close contact. A similar 1,4 short contact between S and Se atoms has been characterized in the structure of **2** with S···Se distance of 3.199 Å (Boryczka *et al.*, 2001). The nonbonding selenium–sulfur interaction and its importance in asymmetric synthesis were observed in arylselenenyl halides (Tiecco *et al.*, 2006).

As a result of interaction between S1 and Se1 the corresponding adjacent outer angles are enlarged. The angles C1–C2–S1 [123.14(13)°] and C9–C3–Se1 [120.87(12)°] are clearly larger than neighboring angles C3–C2–S1 [119.02(13)°] and C2–C3–Se1 [119.82(13)°], respectively.

There are no direction-specific intermolecular interactions between adjacent molecules in the structure of compound **3**. In particular, C–H···N hydrogen bonds are absent, so that the structure consists of effectively isolated molecules. Probably it may be caused by the awkward shape of the title molecule that does not allow to create efficient crystal packing and to generate hydrogen bonding at the same time.

The shortest distances between quinoline rings from different pairs occur for C19–C19 (symmetry code: x, ½ − y, −½ + z): 3.186(2) Å, N1–C17 (symmetry code: 1 + x, y, z): 3.308(2) Å, S1–C14 (symmetry code: −x, −y, −z): 3.553(2) Å, C15–C1 (symmetry code: 1 − x, −y, 1 −z): 3.662(2) Å and C12 – S1 (symmetry code: x, y, −1 +z): 3.897(2) Å.

Antiproliferative activity

Compound **3** was tested for its antiproliferative activity in vitro against four human cancer cell lines: lung cancer (A549), colon cancer (SW707), bladder cancer (HCV29T), breast cancer (T47D). The results of cytotoxic activity in vitro were

expressed as an ID_{50} (μg/ml), i.e., the concentration of compound, which inhibits the proliferation of 50% of tumor cells compared with the control untreated cells. Cisplatin was applied as a referential cytotoxic agent (positive test control). A value <4 μg/ml is considered as an antiproliferative activity criterion for synthetic compounds. The results are summarized in Table 1; previously reported data for compounds **1** and **2** are included for comparison (Boryczka *et al.*, 2002a, b).

The data show that compound **2** exhibits high anticancer activity in vitro against the cells of all human cancer lines applied with ID_{50} values comparable to those of cisplatin. Compound **1** revealed relatively moderate cytotoxic activity with ID_{50} values ranging from 5.7 to 18.4 μg/ml. It is important to note that compound **3** does not show any significant activity (ID_{50} >100 μg/ml) in the concentration range applied.

Molecular electrostatic potential analysis

The electrostatic potential is a powerful tool that has provided insights into molecular properties of small molecules and intermolecular association as well as action of drug molecules and their analogs (Murray *et al.*, 1991; Politzer *et al.*, 1985; Weiner *et al.*, 1982; Marin *et al.*, 2008).

It is a scalar field that can be calculated from the expression:

$$V(r) = \sum \frac{Z_A}{/R_A - r/} - \int \frac{\rho(r')dr'}{/r' - r/}$$

where $\rho(r')$ is the electronic density function obtained from the standard electronic wave function.

In this work, the electrostatic potentials in the surrounding of the molecule and the color-coded computer graphics representation of the molecular isopotential surfaces for molecules **1**, **2**, and **3**, with the equilibrium geometrics in the gaseous phase, have been determined. The optimized gaseous structures were calculated using GAUSSIANW03 program (Gaussian 03, Revision C.02; Frisch *et al.*, 2004). The DFT (Density Functional Theory) at level B3LYP/6 − 311 + G(d.p) was applied and Berny optimization under tight convergence criteria was used. Initial molecular geometry was taken from the X-ray experimental data for each of the molecule. All optimized structures showed positive harmonic vibrations; this meant that a true energy minimum was reached in all performed structure calculations. These geometries were used to compute electrostatic potential V(r) and the electronic densities, which defined the molecular surfaces. Atomic charges were calculated using Charges-from-Electrostatic-Potential, Grid Method (CHELPG), giving charges fit to the electrostatic potential. The MEPs were visualized with Gauss View 4.0 program.

Figure 3a–c show calculated electrostatic potentials for compounds **1**, **2** and **3**, respectively. The total SCF electron density was calculated for the isovalue density of 0.0004 and surface was painted according to the value of the electrostatic potential, i.e., the more red an area is, the more negative electrostatic potential, and the more blue an area is, the more positive electrostatic potential. The projection of the electrostatic potential into a plane of the quinoline ring was plotted for a series of isovalue.

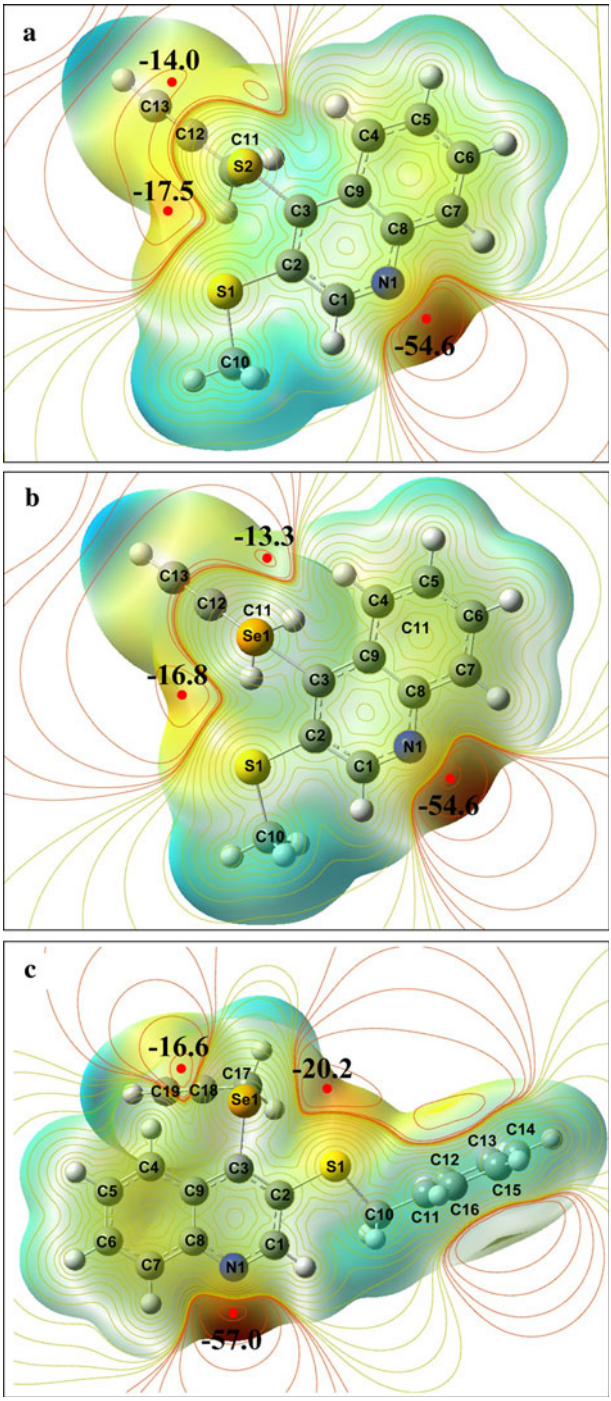
a
-14.0
C13
C12
C11
S2
-17.5
C4
C5
C6
C9
C3
C7
C8
C2
S1
C1
N1
-54.6
C10
b
-13.3
C13
C12
C11
Se1
-16.8
C4
C5
C6
C11
C9
C3
C7
C8
C2
N1
S1
C1
-54.6
C10
c
-16.6
C17
C19
C18
Se1
-20.2
C13
C14
C12
C4
C3
S1
C5
C9
C2
C15
C10
C11
C16
C6
C8
C1
C7
N1
-57.0

◀ **Fig. 3** Color-coded computer graphics representations of the electrostatic potentials of compounds **1** (**a**), **2** (**b**), and **3** (**c**), respectively. The more red an area is, the more negative V(r) and the more blue an area is, the more positive V(r). Projections are in the plane of quinoline ring. The positions of the potential minima (in kcal/mol) are indicated. (Color figure online)

For compound **1** (Fig. 3a), one can observe three main areas of negative electrostatic potential. The first comprises nitrogen atom and carbocyclic ring of the quinoline core with the value of potential minimum equal to −54.6 kcal/mol centered close to nitrogen. This is the most negative value and is associated with the nitrogen lone pair. The potential is strongly negative above and below the aromatic rings, reflecting the presence of π electrons. The other two areas include proximity of sulfur atoms and the triple bond of the propargyl group with the potential minima equal to −17.5 kcal/mol and −14.0 kcal/mol, respectively. In those regions where V(r) is negative the effect of electrons predominates and these are accordingly attractive to an approaching electrophile. Similar arrangement of potentials is seen for molecule **2** in Fig. 3b; however, one can observe changes in the proximity of nonbonded 1,4 S–Se contact and near the triple bond of the propargyl group. The local potential minima for compound **2** are −54.6 kcal/mol, −16.8 kcal/mol, and −13.3 kcal/mol, respectively. For compound **3** (Fig. 3c), the following three main local minima of electrostatic potential can be seen: near the nitrogen atom (−57.0 kcal/mol), the proximity to the 1,4 S–Se quasi-ring (−20.2 kcal/mol), and the proximity to the triple bond of the propargyl group (−16.6 kcal/mol), which is now separately located due to the distinct spatial configuration of the propargyl group.

The electrostatic potential minima are associated with the reactive centers of the molecules **1**–**3**. For compounds **1** and **2**, the most negative region (−54.6 kcal/mol) is involved in formation of short C–H···N hydrogen bonds, whereas the other two regions, which are associated with the nonbonded 1,4 S–Se(S) contact and the propargyl triple bond, are less negative for compound **2** than **1**. Molecule **3** shows three potential minima, none of them is involved in hydrogen bonding and the compound does not show any significant cytotoxic activity. As shown in Table 3, compound **2** containing selenopropargyl group, exhibits the highest antiproliferative activity compared with **1** and **3**. The presented results suggest that there is a relationship between the cytotoxic activity and the regions associated with the structure-dependent electrostatic potential minima. Less negative potential minima give weaker nucleophilic properties of the compound. Formation of one, strong and short H-bond by the reactive center with the most negative potential is the first favorable event in the course of high cytotoxic activity. The second is a reduction in the negative potential minima located near 1,4 S···Se/S contact and the propargyl triple bond. This reduction can be achieved by the substitution of selenium into the propargyl group. Also important is the spatial orientation of the propargyl group. The orientation parallel to the Se1–C3 bond is preferred to achieve less negative potential minima, i.e., −13.3 kcal/mol and −16.8 kcal/mol, respectively (Fig. 3b). For compound **3** (Fig. 3c), the propargyl group is oriented almost perpendicularly to the Se1–C3 bond and the potential minima are significantly higher, i.e., −16.6 kcal/mol and −20.2 kcal/mol, respectively.

The charges derived from the CHELPG methode allowed us to analyze atomic charge distribution over atoms of the 1,4 S···Se(S) quasi-ring and the propargyl

Table 3 Atomic charge distribution over selected atoms of the 1,4 S···Se/S quasi-ring and the propargyl group, main electrostatic potential minima, and the antiproliferative activity in vitro for compounds **1–3**

1	**2**	**3**
1.4 S···Se/S semi-ring group		
S1 −0.193	S1 −0.246	S1 −0.263
C2 −0.114	C2 −0.183	C2 −0.199
C3 +0.247	C3 +0.309	C3 +0.349
S2 −0.227	Se1 −0.128	Se1 −0.143
Propargyl group		
C11 +0.361	C11 + 0.281	C17 +0.278
C12 −0.032	C12 − 0.006	C18 −0.072
C13 −0.348	C13 − 0.362	C19 −0.365
Main electrostatic potential minima [kcal/mol]		
−17.5	−16.8	−20.2
−54.6 (H)	−54.6 (H)	−57.0
−14.0	−13.3	−16.6
Antiproliferative activity		
Moderate	High	Lack

(H) means the hydrogen-bond occupied center

group. Computational results indicate that the intramolecular nonbonded 1,4 S···Se contact (compounds **2** and **3**) is involved in the electrostatic interaction between S and Se atoms, which are both negatively charged. The net charge located on Se is lower compared with the charge of S (Table 3). Substitution of the Se by S (see compound **1** and Table 3) leads to the considerable changes in charge distribution over atoms of the 1,4 S···S quasi-ring, but the distance between S1 and S2 atoms is almost the same. Selenium influences also charge distribution over atoms in the propargyl group, especially charge located on carbon atom involved in the triple-bond formation.

Conclusions

X-ray structure and the molecular electrostatic potential studies performed for the title compound **3** as well as comparative structure-activity analysis for compounds **1–3** allowed for the determination of the main structural features, which are favorable for higher cytotoxic activity of the propargyl thioquinoline compounds. It has been found that spatial orientation of the propargyl group and the substitution of the Se into this group significantly influence the structural arrangement of the electrostatic potential minima, which are responsible for the reactive behavior of the molecules tested. Formation of one short and strong H-bond could be a favorable event in the course of antiproliferative activity. The atomic charges fitted to the electrostatic potential surfaces revealed the selenium influence on charge distribution over atoms of the propargyl group and the intramolecular electrostatic repulsive selenium–sulfur interaction.

Results of the X-ray structure analysis performed for the title compound **3** highlighted the influence of spatial orientation of the propargyl group on the

molecular reactive centers. The presented results can be of interest especially with regard to the synthesis of biologically active enediyne antitumor antibiotics or similar model molecules.

Experimental

General techniques

Melting points were determined in open capillary tubes on a Boetius melting point apparatus and are uncorrected. The ^{1}H-(500 MHz) and ^{13}C-(125 MHz) NMR spectra were recorded on Bruker AMX-500 spectrometer; chemical shifts are referenced to the residual solvent signal ($CDCl_3$, $\delta_H = 7.26$, $\delta_C = 77.0$). Homonuclear ^{1}H connectivities were determined by performing COSY experiments. One-bond heteronuclear ^{1}H-^{13}C connectivities were determined by HMQC experiments. Two- and three-bond ^{1}H-^{13}C connectivities were determined by HMBC experiments optimized for a ^{2,3}J of 10 Hz. EI MS spectra were run on a a Finnigan MAT 95 spectrometer. Elemental C, H, N, S analyses were obtained on a Carlo Erba Model 1108 analyzer.

Synthesis of 3-benzylthio-4-propargylselenoquinoline **3**

A mixture of 4-chloro-3-benzylthioquinoline **4** (0.57 g, 2.0 mmol), selenourea (0.26 g, 2.1 mmol), and 99.8% ethanol (8 ml) was stirred at room temperature for 30 minutes. The reaction mixture was poured into 20 ml of 5% aqueous sodium hydroxide. Propargyl bromide (0.28 g, 2.4 mmol) was added dropwise to the aqueous layer, and the mixture was stirred for 15 minutes. The resultant solid was filtered off and air-dried to give a crude product, which was purified by column chromatography [silica gel 60, <63 μm (Merck) using a mixture of chloroform and ethanol (30:1, v/v) as an eluent] and then crystallized from benzene-hexane to give 0.48 g (65 %) of **3** with m.p. 116–117°C. ^{1}H NMR (in the NMR spectrum, we applied systematic numbering according to IUPAC rules) ($CDCl_3$, 500 MHz) δ: 2.09 (t, J = 2.5 Hz, 1H, CH), 3.53 (d, J = 2.5 Hz, 2H, CH_2Se), 4.32 (s, 2H, CH_2S), 7.59 (m, $^{3}J_{(5,6)} = 8.3$ Hz, $^{3}J_{(6,7)} = 6.9$ Hz, $^{4}J_{(6,8)} = 1.4$ Hz, 1H, H-6), 7.66 (m, $^{3}J_{(7,8)} = 8.3$ Hz, $^{3}J_{(6,7)} = 6.9$ Hz, $^{4}J_{(5,7)} = 1.5$ Hz, 1H, H-7), 8.05 (dd, $^{3}J_{(7,8)} = 8.3$ Hz, $^{4}J_{(6,8)} = 1.4$ Hz, 1H, H-8), 8.51 (dd, $^{3}J_{(5,6)} = 8.3$ Hz, $^{4}J_{(5,7)} = 1.4$ Hz, 1H, H-5), 8.79 (s, 1H, H-2). ^{13}C NMR ($CDCl_3$, 125 MHz) δ: 145.98 (C-2), 139.52 (C-3), 135.26(C-4), 130.30 (C-4a), 127.64 (C-5), 128.00 (C-6), 128.64 (C-7), 129.88 (C-8), 145.64 (C-8a), 12.53 (CH_2), 79.69 (CH_2–*C*), 72.48 (*C*H), 16.56 (CH_3). EI MS (15 eV) m/z (rel. intensity) 369 (M^+, 42), 278 (86). *Anal*. Calcd for $C_{19}H_{15}NSSe$: C 61.95, H 4.10, N 3.80, S 8.70. Found: C 61.88, H 4.22, N 3.71, S 8.65.

X-ray diffraction experiment

The single crystal X-ray experiments were performed at 150 K. For these measurements, a colorless, small, single crystal (0.09 × 0.06 × 0.03 mm^3) of

good quality was preselected under a polarizating microscope. The crystal was mounted on a quartz glass capillary and cooled by a cold, dry, nitrogen gas stream (Oxford Cryosystems equipment). The temperature stability of the measurement was ±0.1 K. The X-ray measurements were performed with Oxford Diffraction

Table 4 Crystallographic data and refinement details for compound **3**. Crystallographic data – CCDC 710965

Crystal data	
Chemical formula	$C_{19}H_{15}NSSe$
Cell setting, space group	Monoclinic, $P2_1/c$
Temperature (K)	150
a (Å)	8.3700(17)
b (Å)	34.735(7)
c (Å)	5.4980(11)
β (°)	97.29(3)
V (Å^3)	1585.5(6)
Z	4
D_x (Mg m^{-3})	1.543
Radiation type	Mo $K\alpha$
μ (mm^{-1})	2.495
Crystal form, color	Needle, colorless
Crystal size (mm)	0.09 × 0.06 × 0.03
Data collection	
Diffractometer	KM4 CCD Sapphire3
Data collection method	$\Delta\omega$–scan
Absorption correction	Multiscan
No. of reflections	
Measured	15506
Independent	5338
Observed	3122
Criterion for observed reflections	$I > 2\sigma(I)$
R_{int}	0.042
θ_{max} (°)	32.72
Refinement	
Refinement on	F^2
$R[F^2 > 2\sigma(F^2)]$	0.0336
$wR(F^2)$	0.0488
S	0.999
No. of reflections	5338
No. of parameters	199
Weighting scheme	Calculated $w = 1/[\sigma^2(F_o^2) + (0.0533P)^2 + 0.1207P]$ where $P = (F_o^2 + 2F_c^2)/3$
$(\Delta/\sigma)_{max}$	<0.0001
$\Delta\rho_{max}$, $\Delta\rho_{min}$ (eÅ^{-3})	0.511, −0.331

KM4 kappa diffractometer equipped with a Sapphire3 CCD detector and graphite-monochromated Mo K_α radiation ($\lambda = 0.71073$ Å). During data collection, ω scans were performed. Multiscan absorption correction was used. Accurate cell parameters (Table 4) were determined and refined using the program CrysAlis CCD. For the integration of the collected data, the program CrysAlis RED was used (Oxford Diffraction, 2006). The structure was first solved using the direct method with SHELXS-97 software, and then the solution was refined with SHELXL-97 (Sheldrick, 2008). All nonhydrogen atoms were refined with anisotropic temperature factors. Aromatic H atoms were treated as riding on their parent C atoms with C–H = 0.95 Å and with Uiso(H) = 1.2Ueq(C). Methylene H atoms also were treated as riding on their parent C atoms with C–H = 0.99 Å and with Uiso(H) = 1.2Ueq(C). Acetylenic H atom was treated as riding on its parent C atom too with C–H = 0.95Å and with Uiso(H) = 1.2Ueq(C). More crystallographic, experimental, and computational details are given in Table 4.

The crystal structure has been deposited at the Cambridge Crystallographic Data Centre and allocated the deposition number: CCDC 710965.

Antiproliferative activity testing

Compound **3** was tested in SRB assay for their antiproliferative activity in vitro against four human cancer cell lines: A549 (lung cancer), SW707 (colon cancer), HCV29T (bladder cancer), T47D (breast cancer) with ID_{50} >100 μg/ml, following published procedures (Boryczka *et al.*, 2002a, b; Mól *et al.*, 2006, 2008). Cisplatin was applied as a referential cytotoxic agent (positive test control). A value <4 μg/ml is considered as an antiproliferative activity criterion for synthetic compounds.

Acknowledgments This work was supported by the Polish Ministry of Science and Higher Education, Grant No. N405 036 31/2655.

References

Aboul-Fadl T (2005) Selenium derivatives as cancer preventive agents. Curr Med Chem Anti-Cancer Agents 5:637–652

Allen FH (2002) The Cambridge structural database: a quarter of a million crystal structures and rising. Acta Cryst B 58:380–388

Bondi A (1964) Van der Waals volumes and radii. J Phys Chem 68:441–451

Boryczka S, Schreurs AMM, Kroon J, Steiner T (2000a) C≡C–H···N hydrogen bonding in 3-methylthio-4-propargylthioquinoline. Acta Cryst C 56:263–264

Boryczka S, Schreurs AMM, Kroon J, Steiner T (2000b) Bis(4-propargyloxy-3-quinolylthio)methane. Acta Cryst C 56:1234–1235

Boryczka S, Rozenberg MS, Schreurs AMM, Kroon J, Starikov EB, Steiner T (2001) A short C-H···N hydrogen bond with a very strong IR spectroscopic effect. New J Chem 9:1111–1113

Boryczka S, Wietrzyk J, Nasulewicz A, Pełczyńska M, Opolski A (2002a) New propargyl thioquinolines-synthesis, antiproliferative activity in vitro structure-activity relationships. Pharmazie 57:733–739

Boryczka S, Wietrzyk J, Opolski A (2002b) Synthesis and antiproliferative activity in vitro of new propargyl thioquinolines. Pharmazie 57:151–154

Davies JE, Bond AD (2001) Quinoline. Acta Cryst E 57:o947–o949

Duann Y-F, Liao Y-J, Guo W, Chang S-M (2003) The characteristic of photoluminescence of tris-(7-substituted-8-hydroxyquinoline) aluminum complexes and polymeric complexes. Appl Organomet Chem 17:952–957

Fitchett CM, Richardson C, Steel PJ (2005) Solid state conformations of symmetrical aromatic biheterocycles: an X-ray crystallographic investigation. Org Biomol Chem 3:498–502

Frisch MJ, Trucks GW, Schlegel HB, Scuseria GE, Robb MA, Cheeseman JR, Montgomery JA, Vreven T, Kudin KN, Burant JC, Millam JM, Iyengar SS, Tomasi J, Barone V, Mennucci B, Cossi M, Scalmani G, Rega N, Petersson GA, Nakatsuji H, Hada M, Ehara M, Toyota K, Fukuda R, Hasegawa J, Ishida M, Nakajima T, Honda Y, Kitao O, Nakai H, Klene M, Li X, Knox JE, Hratchian HP, Cross JB, Bakken V, Adamo C, Jaramillo J, Gomperts R, Stratmann RE, Yazyev O, Austin AJ, Cammi R, Pomelli C, Ochterski JW, Ayala PY, Morokuma K, Voth GA, Salvador P, Dannenberg JJ, Zakrzewski VG, Dapprich S, Daniels AD, Strain MC, Farkas O, Malick DK, Rabuck AD, Raghavachari K, Foresman JB, Ortiz JV, Cui Q, Baboul AG, Clifford S, Cioslowski J, Stefanov BB, Liu G, Liashenko A, Piskorz P, Komaromi I, Martin RL, Fox DJ, Keith T, Al-Laham MA, Peng CY, Nanayakkara A, Challacombe M, Gill PMW, Johnson B, Chen W, Wong MW, Gonzalez C, Pople JA (2004) Gaussian 03, Revision C.02. Gaussian Inc, Wallingford CT

Gensmantel, N. P (2001) In: King FD (ed) Medicinal chemistry: principles and practice. Royal Society of Chemistry, Cambridge, pp 98–129

Gredicak M, Jeric I (2007) Enediyne compounds–new promises in anticancer therapy. Acta Pharm 57:133–150

Grissom JW, Gunawardena GU, Klingberg D, Huang D (1996) The chemistry of enediynes, enyne allenes and related compounds. Tetrahedron 52:6453–6518

Jones GB, Found FS (2002) Designed enediyne antitumor agents. Curr Pharm Design 8:2415–2440

Marin RM, Aguirre NF, Daza EE (2008) Graph theoretical similarity approach to compare molecular electrostatic potentials. J Chem Inf Model 48:109–118

Maślankiewicz A, Boryczka S (1993) Reactions of 4-methoxy-3-quinolinyl and 1,4-dihydro-4-oxo-3-quinolinyl sulfides aiming at the synthesis of 4-chloro-3-quinolinyl sulfides. J Heterocycl Chem 30:1623–1628

Mott AW, Barany G (1984) Synthesis and characterisation of bis[(methylthio)carbonyl]polysulphanes. J Chem Soc Perkin Trans I 2615–2621

Mól W, Naczyński A, Boryczka S, Wietrzyk J, Opolski A (2006) Synthesis and antiproliferative activity in vitro of diacetylenic thioquinolines. Pharmazie 61:742–746

Mól W, Matyja M, Filip B, Wietrzyk J, Boryczka S (2008) Synthesis and antiproliferative activity in vitro of novel (2-butynyl)thioquinolines. Bioorg Med Chem 16:8136–8141

Murray JS, Lane P, Brinck T, Politzer P (1991) Electrostatic potentials on the molecular surfaces of cyclic ureides. J Phys Chem 95:844–848

Nicolaou KC, Dai W-M (1991) Chemistry and biology of the enediyne anticancer antibiotics. Angew Chem Int Ed 30:1387–1416

Oxford Diffraction (2006) CrysAlis CCD and CrysAlis RED. Versions 1.171.29. Oxford Diffraction Ltd, Wrocław, Poland

Politzer P, Laurence PR, Jayasuriya K (1985) Molecular electrostatic potentials: an effective tool for the elucidation of biochemical phenomena. Environ Health Perspect 61:191–202

Sheldrick GM (2008) A short history of SHELX. Acta Cryst A 64:112–122

Skrzypek L, Suwińska K (2002) The preparation of the stable tautomers of 4-mercapto-3-quinolinesulfonic and 1,4-dihydro-4-thioxo-3-quinolinesulfonic acids. Heterocycles 57:2035–2044

Tiecco M, Testaferri L, Santi C, Tomassini C, Santoro S, Marini F, Bagnoli L, Temperini A, Costantino F (2006) Intramolecular nonbonding interactions between selenium and sulfur–spectroscopic evidence and importance in asymmetric synthesis. Eur J Org Chem 4867–4873

Weiner PK, Langridge R, Blaney JM, Schaffer R, Kollman PA (1982) Electrostatic potential molecular surfaces. Proc Natl Acad Sci USA 79:3754–3758